Research Article

Cancer Immunology Research

PD-L1 Binds to B7-1 Only *In Cis* on the Same Cell Surface

Apoorvi Chaudhri, Yanping Xiao, Alyssa N. Klee, Xiaoxu Wang, Baogong Zhu, and Gordon J. Freeman

Abstract

Programmed death ligand 1 (PD-L1)–mediated immunosuppression regulates peripheral tolerance and is often co-opted by tumors to evade immune attack. PD-L1 binds to PD-1 but also binds to B7-1 (CD80) to regulate T-cell function. The binding interaction of PD-L1 with B7-1 and its functional role need further investigation to understand differences between PD-1 and PD-L1 tumor immunotherapy. We examined the molecular orientation of PD-L1 binding to B7-1 using cell-to-cell binding assays, ELISA, and flow cytometry. As expected, PD-L1–transfected cells bound to PD-1–transfected cells, and B7-1 cells bound to CD28 or CTLA-4–transfected cells; however, PD-L1 cells did not bind to B7-1 cells. By ELISA and flow cytometry with purified proteins, we found PD-L1 and B7-1 had a strong binding interaction only when PD-L1 was flexible. Soluble PD-1 and B7-1 competed for binding to PD-L1. Binding of native PD-L1 and B7-1 *in cis* on the same cell surface was demonstrated with NanoBiT proximity assays. Thus, PD-L1–B7-1 interaction can occur *in cis* on the same cell but not *in trans* between two cells, which suggests a model in which PD-L1 can bend via its 11-amino acid, flexible stalk to bind to B7-1 *in cis*, in a manner that can competitively block the binding of PD-L1 to PD-1 or of B7-1 to CD28. This binding orientation emphasizes the functional importance of coexpression of PD-L1 and B7-1 on the same cell. We found such coexpression on tumor-infiltrating myeloid cells. Our findings may help better utilize these pathways in cancer immunotherapy. *Cancer Immunol Res; 6(8); 921–9. ©2018 AACR.*

Introduction

Programmed death 1 (PD-1, CD279) and its ligand programmed death ligand 1 (PD-L1, B7-H1, CD274) are promising targets in cancer immunotherapy (1, 2). Immunosuppression mediated by PD-L1 is a mechanism of tumor immune evasion. PD-L1 exerts its function through several possible mechanisms. It can interact with PD-1 to tolerize T cells (3–5), render cells resistant to $CD8^+$ T-cell and Fas ligand–mediated lysis (6, 7), or regulate the development of induced regulatory T cells and maintain their function (8).

Our previous studies identified PD-L1 as a ligand for B7-1 using COS cell expression cloning that showed PD-L1–transfected cells bound to B7-1-Ig immobilized on plates coated with anti-Ig (9). Biacore studies determined K_Ds of 0.77 and 1.4 μmol/L for the binding of human PD-L1 to PD-1 and B7-1, respectively (9, 10). Other investigators confirmed this interaction using biotin-conjugated B7-1-Ig to show soluble B7-1 binding to PD-L1–transfected 293T cells by flow cytometry (11). However, another study using Biacore showed weaker interactions with K_Ds of 7.8 and 18.8 μmol/L for the binding of human PD-L1 to PD-1 and B7-1, respectively (12). Here, we examine the orientation of the molecules that will allow strong and functionally relevant interactions. We examined cell-to-cell binding of ligands and receptors using transfected cells in a cell conjugation assay (13). We found that PD-L1–transfected cells did not bind to B7-1–transfected cells, suggesting that the structural orientation of PD-L1 and B7-1 is not compatible with binding *in trans* between two cells. However, when PD-L1 was presented in a more accessible and flexible form, a strong interaction between PD-L1 and B7-1 was observed. This was confirmed using two separate approaches of ELISA and flow cytometry. These results failed to confirm a *trans* interaction but suggested a *cis* interaction. We cotransfected PD-L1 and B7-1 in the same cell and, using a proximity assay (NanoBiT), confirmed a *cis* binding interaction. Our results indicate binding between PD-L1 and B7-1 in *cis* on the same cell surface but not *in trans* between two cells. We further distinguish the binding region of PD-L1 to B7-1 as being overlapping but higher on the GFCC′C″ face of the PD-L1 IgV domain than the binding surface for PD-1. Together, our study offers molecular insight into the PD-L1 pathway.

Materials and Methods

Cells and culture media

Mouse 300.19 cells are an Abelson mouse leukemia virus transformed pre–B-cell line from Swiss Webster mice that grows as a nonadherent, single-cell suspension. The mouse EL4 T-cell line was obtained from ATCC. The 300.19 cells, 300.19 PD-L1–transfected cells, 300.19 PD-L1-IgV-Tim-3 mucin domain–transfected cells, and EL4 cells were transfected by electroporation

Department of Medical Oncology, Dana-Farber Cancer Institute, Harvard Medical School, Boston, Massachusetts.

Note: Supplementary data for this article are available at Cancer Immunology Research Online (http://cancerimmunolres.aacrjournals.org/).

A. Chaudhri and Y. Xiao contributed equally to this article.

A. Chaudhri and Y. Xiao are co-first authors of this article.

Corresponding Author: Gordon J. Freeman, Dana-Farber Cancer Institute, 450 Brookline Avenue, Boston, MA 02115. Phone: 617-632-4585; Fax: 617-632-5167; E-mail: Gordon_Freeman@dfci.harvard.edu

doi: 10.1158/2326-6066.CIR-17-0316

with mouse or human PD-L1, B7-1, PD-1, CD28, CTLA-4, or other appropriate construct cDNA in the pEF-Puro or pEF6-Blasticidin expression vectors in our laboratory. Cells were selected in media containing puromycin or blasticidin, sorted with specific mAbs, and subcloned. Cell-surface expression of the indicated molecules was verified by flow cytometry using specific mAbs. Cells were cultured no more than 4 months before new thaws, but have not been reauthenticated within the past year. Cells were cultured at 37°C with 5% CO_2 in RPMI1640 (Mediatech) supplemented with 10% heat-inactivated FBS (Invitrogen), 1% streptomycin/penicillin, 15 μg/mL gentamicin (Invitrogen), 1% GlutaMAX (Invitrogen), 50 μmol/L β-mercaptoethanol (Sigma-Aldrich), and 5 μg/mL puromycin or blasticidin. The same media minus β-mercaptoethanol were used for EL4 cells. COS cells were cultured at 37°C with 10% CO_2 in DMEM (Mediatech) supplemented with 10% heat-inactivated FBS (Invitrogen), 1% streptomycin/penicillin, 15 μg/mL gentamicin (Invitrogen), 1% GlutaMAX (Invitrogen).

COS cell transfection

COS cells were plated on day 1 to reach 40% to 60% confluency on the day of transfection. Transfection was performed on day 2 using a 3:1 ratio of GeneJuice (Novagen) to plasmid. Cells were harvested 48 to 60 hours after transfection and analyzed by flow cytometry.

Fusion proteins

Recombinant proteins human B7-1-hIgG1 and human PD-1-hIgG1 were purchased from R&D systems. Human IgG was purchased from The Jackson Laboratory and Bio X Cell. Mouse IgG1 isotype control antibody (clone MOPC21) was purchased from Bio X Cell. Mouse IgG2b and mouse IgG2a were purchased from Southern Biotech. hPD-1-mIgG2a and hB7-1-mIgG2a were purchased from Chimerigen. hPD-L1-mIgG2a was made in our laboratory (14).

Antibodies

Secondary antibodies absorbed against the other species (mouse or human) were used. Unconjugated and PE-conjugated Goat $F(ab')_2$ anti-mouse IgG2a (absorbed against human Ig), PE-conjugated goat $F(ab')_2$ anti-human IgG (absorbed against mouse Ig), PE-conjugated goat anti-human IgG (absorbed against mouse Ig), and HRP-conjugated goat anti-human IgG (absorbed against mouse Ig) were purchased from Southern Biotech. Antibodies specific for human PD-L1, mouse PD-L1, and human TIM-3 were made in our laboratory (15).

Flow cytometry

Cells were incubated with the indicated primary antibody or fusion protein, washed, and incubated with 10 μg/mL of the appropriate secondary antibody, washed, and analyzed by flow cytometry on a BD FACSCanto II. Data were analyzed using FlowJo 10 software. Half-maximal effective concentration (EC_{50}) values were calculated using 4-parameter variable slope regression curve (Prism 7, GraphPad Software).

ELISA

ELISA plates were coated with 2 μg/mL primary protein in PBS overnight at 4°C, then blocked in 1% BSA and washed in ELISA washing buffer (PBS pH 7.4 with 0.05% Tween 20). Fusion proteins were diluted in PBS plus 1% BSA at the indicated concentrations and incubated with plate-bound ligand for an hour. Bound fusion protein was detected using goat anti-human IgG HRP. EC_{50} values were calculated using 4-parameter variable slope regression curve (Prism 7, GraphPad Software).

Cell conjugation assay

A cell conjugation assay for cell surface receptor–ligand binding was developed in our previous study (13). Briefly, cells transfected with cell surface gene 1 were labeled with the red fluorescent dye PKH26 (Sigma), and cells transfected with cell surface gene 2 were labeled with the green fluorescent dye PKH67 (Sigma). Red dye–labeled and green dye–labeled cells were incubated together as described previously (13). Conjugate formation was analyzed immediately by flow cytometry using the PE channel for the red dye and the FITC channel for the green dye. Data were analyzed using FlowJo 9.5.2 software (TreeStar).

NanoBiT

HEK 293-H cells (Invitrogen) were plated in white 96-well plates (Cornell) to reach 60% to 80% confluency on the day of transfection. On day 2, plasmids were transfected using Fugene Transfection Reagent (Promega). Thirty hours posttransfection, Nano-Glo live cell substrate (Promega) was added to the cells at a 1 to 20 dilution. Immediately after addition, luminescence was assayed using Spectra Max M3 (Molecular Devices). Integration time was 1,500 seconds.

Mutagenesis

A pEF-Puro plasmid containing a chimeric cDNA construct composed of the human PD-L1 signal and IgV domains fused to the human TIM-3 mucin, transmembrane, and cytoplasmic domains was mutagenized using appropriate oligonucleotide primers and In-fusion cloning (16). The plasmids (unmutated or mutated) were transfected into COS cells. After 48 to 60 hours, the cells were harvested and incubated with PD-1-hIg, B7–1-hIg, or human Ig at 5 μg/mL. Binding of fusion protein was detected using flow cytometry with goat anti-human IgG PE. We calculated the binding of PD-1 and B7-1 to mutant PD-L1–transfected cells using the formula:

Binding percentage = A × B × 100

Where A is

[MFI of PD-1 or B7-1 binding to mutant chimera] – [isotype to vector control] ÷

[MFI of PD-1 or B7-1 binding to parent chimera] – [isotype to vector control]

and B normalizes for expression level of the individual construct:

[MFI of TIM-3 mAb binding to parent chimera] – [isotype to vector control] ÷

[MFI of TIM-3 mAb binding to mutant chimera] – [isotype to vector control]

The PD-L1 structure was generated from PDB ID: 3BIS (17) and highlighted using Cn3D software (NCBI).

Mouse tumor experiments

All experiments performed in mice have been approved by the Dana-Farber Institutional Care and Use Committee.

Flow cytometry of tumor-infiltrating myeloid cells

For study of the myeloid population, mice were injected subcutaneously with 0.5×10^6 CT26 colon carcinoma cells per mouse. Mice were sacrificed at tumor size of 1 cm. Tumors were disaggregated using collagenase and red blood cells (RBC) were lysed using RBC lysis buffer. Cells were Fc blocked and stained with fluorochrome-conjugated antibodies for 30 minutes. The live/dead stain used was Zombie/NIR (BioLegend). For intracellular staining, cells were first permeabilized using Foxp3 Transcription Factor Fixation/Permeabilization Concentrate and Diluent solution (eBioscience). The flourochrome-conjugated antibodies used were anti-NOS2 APC (clone CXNFT) from eBioscience, anti-CD45 BV711 (clone 30-F11), anti-CD11c (clone N418), anti-CD11b (clone M1/70), anti-CD274 BV421 (clone 10F.9G2), anti-CD80 BV650 (clone 16-10A1) from BioLegend, and anti-Arg1 Fluorescein from R&D Systems. Acquisition was performed on an LSR Fortessa SORP HTS flow cytometer. Data analysis was performed using FlowJo 10.

Statistical analysis

Results were graphed as mean with SEM. The statistical analysis was performed using GraphPad Prism version 7 as detailed in the figure legends.

Results

PD-L1–transfected cells do not bind to B7-1–transfected cells

To study the binding of PD-L1 to B7-1 on cell surfaces, we used a cell conjugation assay (13). The parental 300.19 cells (300) and transfectants grow as nonadherent single cells. One transfected cell was labeled with a red dye and the other transfected cell with a green dye. The binding of the two cells was assessed by flow cytometry and indicated by double positive events (yellow dots). As expected, double positive events had a higher forward scatter (Fig. 1). The conjugate percentage for negative controls with irrelevant cells was <1% (Fig. 1).

We found that mouse (m) PD-L1–transfected 300 cells did not bind to mB7-1–transfected 300 cells (Fig. 1A). In contrast, mPD-L1–transfected 300 cells bound to mPD-1–transfected 300 cells (Fig. 1B) and mB7-1–transfected 300 cells bound to mCD28-transfected 300 cells (Fig. 1C). As negative controls, mPD-1–transfected 300 cells did not bind to mCD28-transfected 300 cells (Fig. 1D) and mB7-1–transfected 300 cells did not bind to mPD-L2–transfected 300 cells (Fig. 1E). Although the binding affinity of B7-1 to CD28 is lower than that of B7-1 to PD-L1 (4 vs. 1.7 μmol/L; ref. 9), the cell-to-cell binding of B7-1 to CD28 was readily detected, suggesting that the failure to detect B7-1 cell binding to PD-L1 cells was not due to a low binding affinity.

We also observed that human (h) PD-L1–transfected 300 cells did not bind to hB7-1–transfected 300 cells (Fig. 2A), whereas hPD-L1–transfected 300 cells bound to hPD-1–transfected 300 cells (Fig. 2B) and hB7-1–transfected 300 cells bound to hCTLA-4–transfected 300 cells (Fig. 2C). As a negative control, hPD-1–transfected 300 cells did not bind to hCTLA-4–transfected 300 cells (Fig. 2D).

PD-L1–transfected EL4 cells do not bind to B7-1–transfected EL4 cells

To exclude the possibility that PD-L1 and/or B7-1 expressed on B cells may not be folded properly for ligand and receptor binding, we examined the binding with transfected mouse EL4 T cells using the cell conjugation assay. Similar results were obtained with mPD-L1–transfected EL4 cells, which did not bind to mB7-1–transfected EL4 cells (Supplementary Fig. S1A), whereas mB7-1–transfected EL4 cells bound to mCTLA-4–transfected EL4 cells (Supplementary Fig. S1B). As negative controls, mB7-1 or mCTLA-4–transfected EL4 cells did not bind to untransfected EL4 cells (Supplementary Fig. S1C and S1D). The conjugate percentage of mB7-1–transfected EL4 cell binding to mCTLA4-transfected EL4 cells (3.9%; Supplementary Fig. S1B) was lower than that of hB7-1–transfected 300 cell binding to hCTLA-4–transfected 300 cells (13.6%; Fig. 2C), probably due to the larger

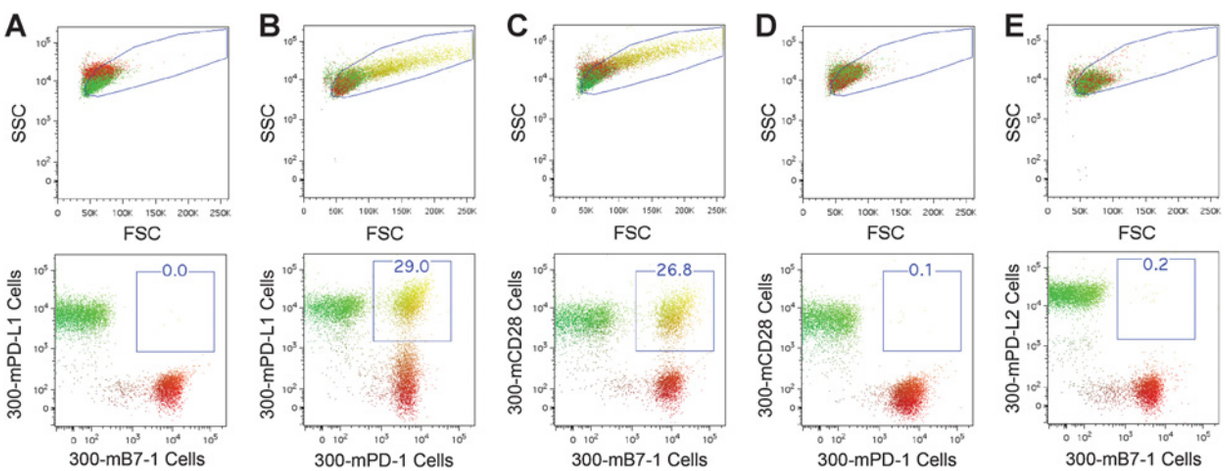

Figure 1.

mPD-L1–transfected 300 cells do not bind to mB7-1–transfected 300 cells. Cell-to-cell binding of the indicated transfected cells was analyzed by cell conjugation assay. **A–E,** The binding of the red dye–labeled cells and the green dye–labeled cells was assessed by flow cytometry and indicated by double positive events (yellow dots). Data are representative of at least four independent experiments.

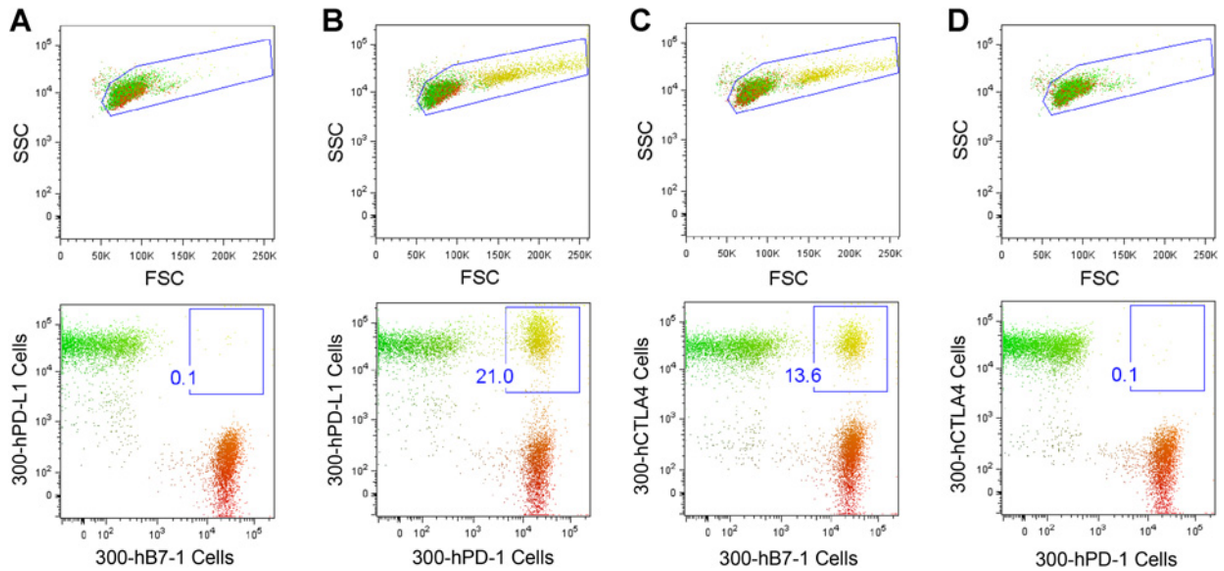

Figure 2.

hPD-L1–transfected 300 cells do not bind to hB7-1–transfected 300 cells. **A–D,** Cell-to-cell binding of the indicated transfected cells was analyzed by cell conjugation assay, as in Fig. 1. Data are representative of two independent experiments.

size of EL4 cells leading to easier disruption of conjugates during the turbulence of flow cytometry.

Taken together, our results with transfected B- and T-cell lines show that the structural orientation of PD-L1 and B7-1 is not compatible with binding *in trans* between two cells (cell surface to cell surface binding).

PD-L1 binds weakly to B7-1 if constrained, but binds strongly if flexible

We extended our binding study to purified proteins in an ELISA format. When hPD-L1-mIgG2a fusion protein was adhered to the plate, it bound weakly to B7-1 with an EC_{50} of 1.6 μg/mL. In contrast, the binding of PD-1 was strong with an EC_{50} of 0.022 μg/mL (Fig. 3A).

We next tested binding in an assay where the ligand Ig fusion protein has a greater degree of freedom by first coating the plate with goat anti-mIgG2a and then capturing the hPD-L1-mIgG2a fusion protein. In this flexible format, the binding affinity of B7-1 was stronger than in the standard ELISA format with an EC_{50} of 0.059 μg/mL (Fig. 3A). The EC_{50} of PD-1 was similar to the previous assay, 0.014 μg/mL. The original identification of the B7-1 interaction with PD-L1 was by COS cell expression cloning

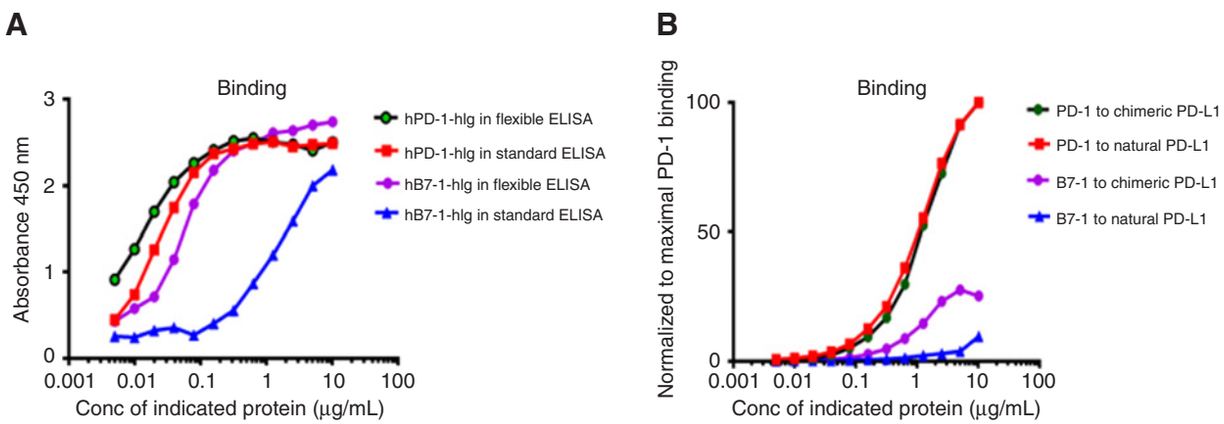

Figure 3.

B7-1 binds weakly to PD-L1 in a standard ELISA or cell surface format but well in a flexible format. **A,** In a standard ELISA, the plate was coated with hPD-L1-mIgG2a at 2 μg/mL. After washing, the indicated concentration of hPD-1-hIg or hB7-1-hIg fusion protein was added. Bound fusion protein was detected using goat anti-human IgG HRP. In a flexible ELISA, the plate was coated with goat anti-mouse IgG2a (2 μg/mL) followed by addition of hPD-L1-mIgG2a (10 μg/mL). After washing, the indicated concentration of hPD-1-hIg or hB7-1-hIg fusion protein was added. Bound fusion protein was detected using goat anti-human IgG HRP. Data are representative of three independent experiments. **B,** 300 hPD-L1–transfected cells and 300 cells transfected with a chimeric cell surface protein composed of the PD-L1 IgV domain and the TIM-3 mucin, transmembrane, and cytoplasmic domain were stained with the indicated concentrations of PD-1-hIg, B7-1-hIg fusion proteins. The secondary antibody was goat anti-human IgG PE. Maximum PD-1 binding to natural PD-L1 = 33,837, maximum PD-1 binding to chimeric PD-L1 = 154,694. Data are representative of two independent experiments.

where the plate was first coated with anti-Ig, followed by B7-1-Ig. Transfected COS cells were captured on this coated plate, a flexible format that corresponds to the flexible ELISA format used in Fig. 3A (9).

We next examined the binding of hB7-1-hIg and hPD-1-hIg fusion proteins to hPD-L1–transfected 300 cells (Fig. 3B). As with the standard ELISA format, we observed PD-L1 bound weakly to B7-1 but strongly to PD-1. The EC_{50} of PD-L1–B7-1 was not determinable and of PD-L1–PD-1 was 1.26 μg/mL. To mimic the flexible ELISA format, we made a flexible cell surface form of PD-L1 by making a chimeric molecule linking the PD-L1 IgV domain to the flexible mucin domain of TIM-3. Both B7-1 (EC_{50}, 1.06 μg/mL) and PD-1 (EC_{50} 1.42 μg/mL) bound well to cell surface hPD-L1 presented in this flexible format (Fig. 3B). As a positive control, we tested the binding of anti-human PD-L1 (clone 29E.2A3) with 300.19 cells transfected with hPD-L1 or hPD-L1-TIM-3 chimera and observed high-affinity binding to both cells (Supplementary Fig. S2). Our data are consistent with the previous finding that only the PD-L1 IgV domain participates in binding with PD-1 and B7-1 (17, 18).

Our results show that B7-1 does not bind well to PD-L1 when the molecules are on two different cells or as purified proteins if one is immobilized. They do bind well as soluble molecules if one is allowed rotational flexibility. PD-L1-TIM-3 chimera–transfected cells bound to B7-1 soluble protein (Fig. 3B), but preliminary experiments showed that PD-L1-TIM-3 chimera–transfected cells did not bind to B7-1–transfected cells. This led us to hypothesize that the molecules needed to be in a parallel orientation to bind, which can be achieved by expression on the same cell surface.

PD-L1 binds with B7-1 on the same cell surface in a *cis* interaction

We tested whether PD-L1 binds with B7-1 on the same cell surface, using a NanoBiT proximity assay system, which uses a split luciferase enzyme. The PD-L1, B7-1, and PD-1 cytoplasmic domains were linked to the Small BIT and Large BIT luciferase peptide sequences. Luminescence is generated only when the Small and Large BIT peptides can come together and form an active luciferase enzyme. This can be achieved only if their molecular partners (B7-1 and PD-L1) stably interact. We detected significant luminescence with PD-L1-Large BIT and B7-1-Small BIT, indicating a binding interaction between them (Fig. 4A and B). As expected, we detected significant luminescence with the B7-1-Large BIT and B7-1-Small BIT combination (Fig. 4A) because B7-1 is known to form a back-to-back homodimer. Negative controls of PD-L1-Large BIT and Halo-Tag Small BIT had negligible luminescence. The interaction between PD-1 and PD-L1 *in cis* was not significantly different from the negative control, indicating that PD-L1 and PD-1 interact weakly *in cis* (Fig. 4A).

Expression of B7-1 and PD-L1 on tumor-infiltrating myeloid cells

We examined the coexpression of B7-1 and PD-L1 on tumor-infiltrating myeloid cells. The tumors were harvested from mice bearing CT26 colon carcinoma with tumors about 1 cm in size. Myeloid cells gated as $CD45^+CD11c^-CD11b^+NOS2^+$ and as $CD45^+CD11c^-CD11b^+Arg1^+$ co-expressed B7-1 and PD-L1 molecules at high levels, 84% and 72%, respectively (Supplementary Figs. S3 and S4).

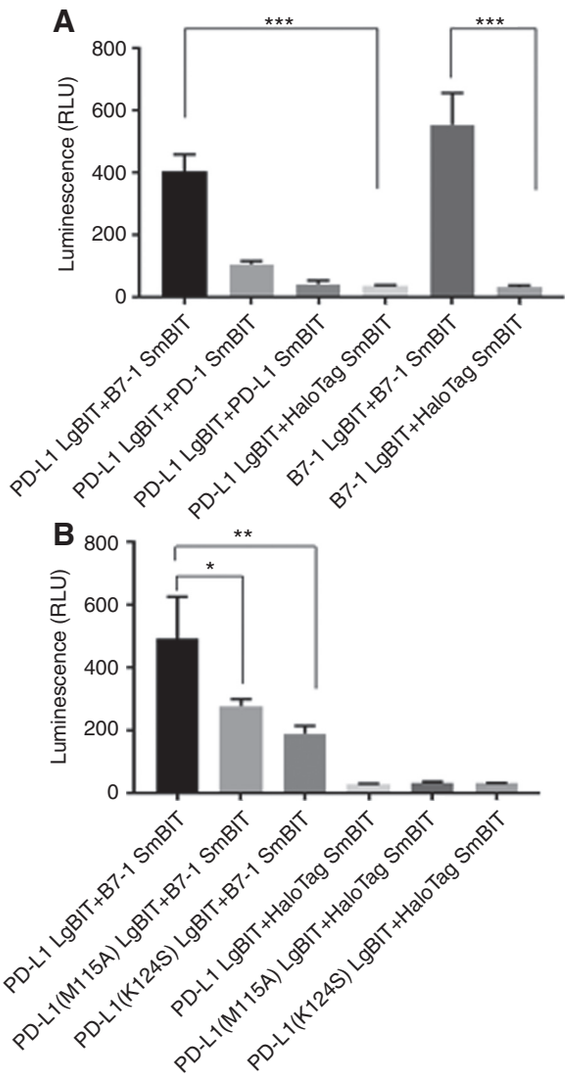

Figure 4.

PD-L1 and B7-1 associate *in cis* on the same cell surface. The indicated B7-1, PD-1, PD-L1, or mutant PD-L1 Small Bit (SmBit) or Large BIT (LgBit) plasmids or Halo Tag-Small Bit as a negative control were transfected into HEK 293-H cells as described in Materials and Methods. Thirty hours after transfection, luminescence was assayed using Nano-Glo Live cell substrate. **A,** Interaction of PD-L1 with B7-1, PD-L1 with PD-1, PD-L1 with PD-L1, and B7-1 with B7-1. Statistical analysis was done using one-way ANOVA and Bonferroni test (***, $P \leq 0.001$). **B,** Interaction of PD-L1 or mutant PD-L1 with B7-1. Statistical analysis was done using one-way ANOVA and Dunnett test (*, $P \leq 0.05$; **, $P \leq 0.01$).

Mutagenesis to localize the binding site of PD-L1 for B7-1

We mutated amino acids in the PD-L1 IgV domain to identify residues that were important for binding to B7-1 or PD-1. The PD-L1-IgV TIM-3 chimeric construct (with the indicated mutations in the PD-L1 IgV domain) was transfected into COS cells and binding of B7-1-hIg or PD-1-hIg was assayed by flow cytometry (Fig. 5A). Binding was normalized to the expression level of the TIM-3 mucin domain, which has the same structure in all constructs, using a TIM-3 mucin-specific mAb. D49K and K124S reduced both B7-1 and PD-1 binding. R113S and M115A reduced B7-1 binding but had less effect on PD-1 binding. E58S, N63A,

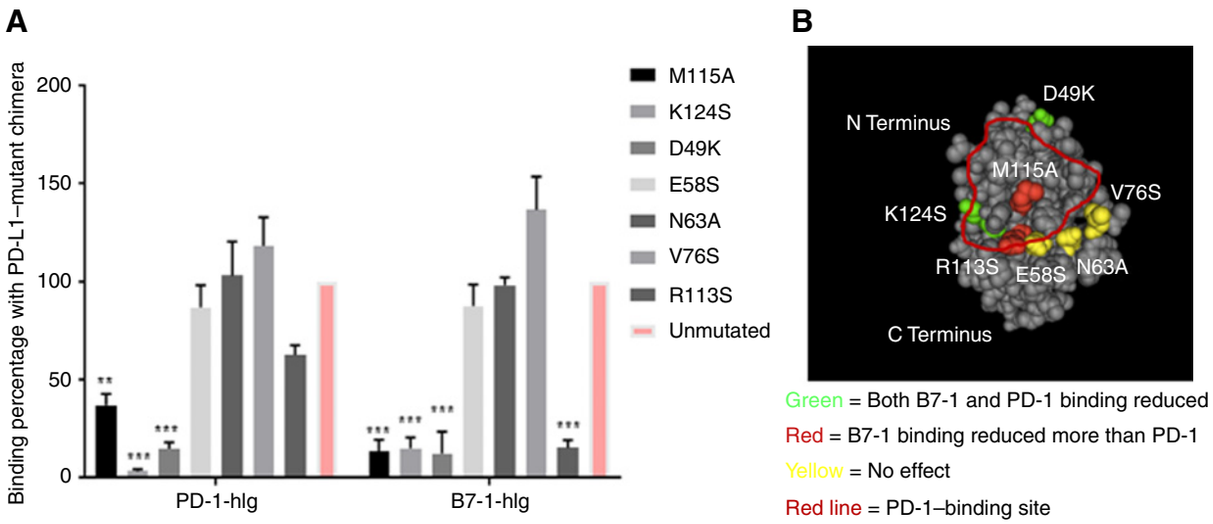

Figure 5.

Amino acid residues in the PD-L1 IgV domain involved in PD-1 and/or B7-1 binding. **A,** Plasmids expressing a chimeric cell surface protein composed of the PD-L1 IgV domain (unmutated or mutated as indicated) and the TIM-3 mucin, transmembrane, and cytoplasmic domain were transfected into COS cells. After 48 to 60 hours, the cells were harvested and incubated with PD-1-hIg, B7-1-hIg, or human-Ig at 5 μg/mL. Binding of fusion protein was detected with goat anti-human IgG PE. Expression of the PD-L1-TIM-3 chimeric protein was detected with anti–TIM-3 specific for the TIM-3 mucin domain and goat anti-mIgG PE, and used to normalize the fusion protein binding as described in the Materials and Methods section. Data are representative of four independent experiments. Statistical analysis was done using one-way ANOVA and Dunnett test (unmutated vs. mutated; **, $P \leq 0.01$; ***, $P \leq 0.001$). Error bars, SEM. **B,** Mutated amino acids and their effect on binding are highlighted on the PD-L1 IgV structure (Lin et al., 2008).

and V76S had no effect on binding. The highlighted crystal structure illustrates the effect of PD-L1-IgV mutations on PD-1 and B7-1 binding (Fig. 5B).

From our studies of PD-L1 IgV domains with M115A or K124S mutations, we observed an 80% decrease in the binding of B7-1-Ig with PD-L1 as measured by flow cytometry as shown in Fig. 5. In our NanoBiT experiment, a similar decrease in binding, as measured by luminescence, was observed with M115A or K124S mutant PD-L1-Large BIT and B7-1-Small BIT (Fig. 4B). These results are consistent with a *cis* interaction between PD-L1 and B7-1 and are not readily explained by a *trans* interaction because this would have the molecules on different membrane surfaces that would not bring the Large and Small BITs into contact.

PD-L1 antibodies block the binding of B7-1 or PD-1 to PD-L1

We examined the capacity of PD-L1 antibodies to block the interaction of PD-L1 with B7-1 or PD-1 in a flow cytometry–based assay using 300-hPD-L1 IgV TIM-3 cells incubated with anti–PD-L1 and either B7-1-hIg or PD-1-hIg. Anti–PD-L1 298B.8E2 blocks both interactions equally well in a concentration-dependent fashion (Fig. 6A). A large panel of mAbs was tested and all human PD-L1 mAb that blocked the PD-1 interaction also blocked the B7-1 interaction (Supplementary Table S1). Our findings are consistent with previous results that the binding site for both PD-L1 and B7-1 on PD-L1 is in the same vicinity (18). Although two independent mouse PD-L1 mAbs have been reported that block only the B7-1 interaction (9, 11), we have not yet identified a human equivalent.

Both B7-1 and PD-1 compete for binding to PD-L1

We performed competition assays between PD-1 and B7-1 to further understand the interactions of the two molecules for binding with PD-L1. We used a flow cytometry–based assay using 300-hPD-L1 IgV TIM-3 cells incubated with a variable amount of one protein and a constant amount of the second protein. B7-1 competed with PD-1 for binding to PD-L1 with an EC_{50} of 4.06 μg/mL (Fig. 6B). Similarly, PD-1 competed with B7-1 for binding to PD-L1 with an EC_{50} of 1.44 μg/mL (Fig. 6C).

A model for interactions among PD-L1, PD-1, B7-1, CD28, and CTLA-4

Crosslinking studies have suggested that the GFCC′C″ faces of the IgV domains of B7-1 and PD-L1 are used for binding to each other as well as their other receptors (PD-1 and CD28/CTLA-4; ref. 9). We propose that PD-L1 can bend via its 11-amino acid, proline-rich flexible stalk to bind to B7-1 *in cis* in a way that can competitively block the binding of PD-L1 to PD-1 or of B7-1 to CD28 (Fig. 7; ref. 9).

Discussion

Our data suggest that the structural orientation of PD-L1 and B7-1 can support binding *in cis* on the same cell surface or of soluble natural PD-L1 or B7-1 to cell surface B7-1 or PD-L1, respectively. In each case, the molecules would bind in parallel orientation. If the PD-1 or B7-1 is part of an Fc fusion protein, binding may be detectable only if the hinge of the Fc construct is flexible and long enough to allow the PD-L1 or B7-1 to be in parallel orientation to its ligand and the Fc not be sterically blocked by the cell surface.

Various studies have investigated the functional role of the B7-1–PD-L1 interaction and conflicting results have been reported. Blockade of the PD-L1–B7-1 interaction breaks T-cell anergy and oral tolerance and in NOD mice accelerated progression to autoimmune diabetes (9, 11, 18, 19). This supports an inhibitory

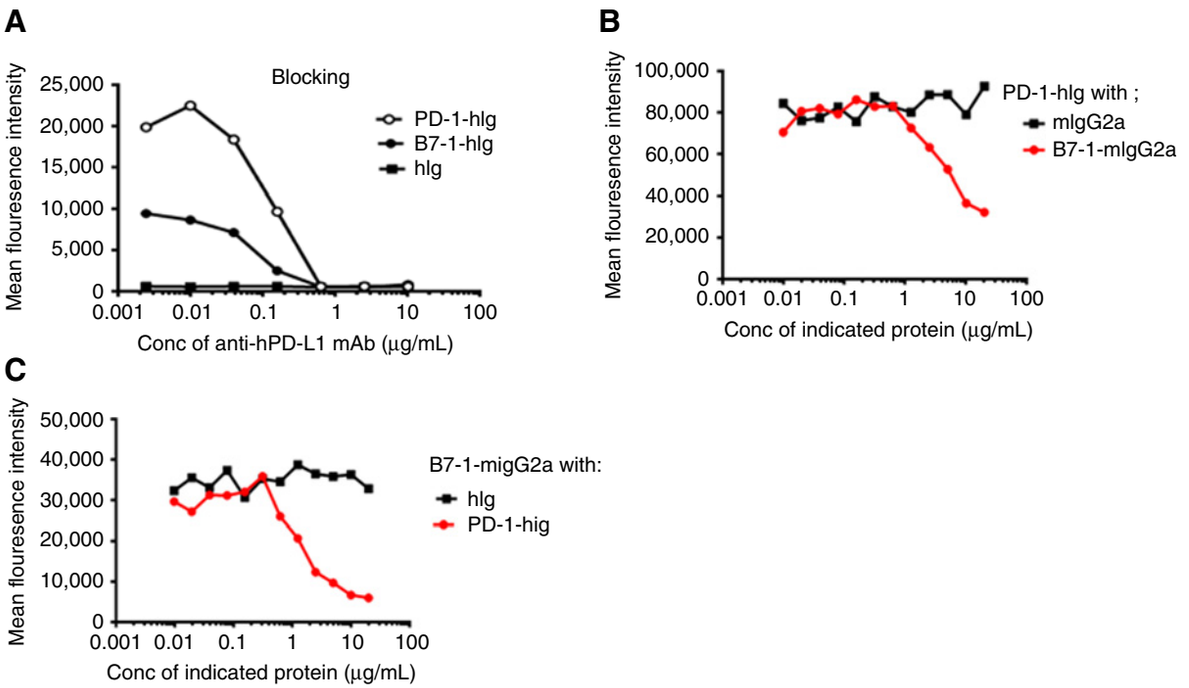

Figure 6.

B7-1 and PD-1 compete for binding to PD-L1. **A,** 300 cells expressing a chimeric cell surface protein composed of the PD-L1 IgV domain and the TIM-3 mucin, transmembrane, and cytoplasmic domain were incubated with the indicated concentrations of anti–PD-L1 298B.8E2 for 30 minutes, followed by 2.5 μg/mL of PD-1-hIg, B7-1-hIg, or control hIg fusion proteins. Binding of fusion protein was detected with $F(ab)_2$ anti-human IgG PE. Data are representative of two independent experiments. **B,** 300 hPD-L1-TIM-3 chimera–transfected cells were incubated with the indicated concentrations of B7-1-mIgG2a or mIgG2a. PD-1-hIg fusion protein was added at 2.5μg/mL. The detection reagent was $F(ab)_2$ anti-hIgG PE. Data are representative of two independent experiments. **C,** 300 hPD-L1-TIM-3 chimera–transfected cells were incubated with the indicated concentrations of hPD-1-hIg or hIg. hB7-1-mIgG2a fusion protein was added at 2.5 μg/mL. The detection reagent was $F(ab)_2$ anti-mIgG2a PE. Data are representative of two independent experiments.

role on T-cell activation. Other studies show coexpression of B7-1 on PD-L1$^+$ tumor cells or show that treatment with a soluble form of B7-1 (B7-1-Ig) overcomes PD-L1–mediated immunosuppression. Mechanistically, this was proposed to work through B7-1 binding to PD-L1 and blocking the interaction of PD-L1 with PD-1 as well as B7-1 binding to CD28 to deliver a costimulatory signal (20–22).

A previous study suggested that B7 on T cells attenuated alloresponses via a T cell–T cell interaction with CTLA-4 (23). This could be B7 binding to CTLA-4 *in cis* on T cells or soluble ligand binding. The binding of soluble B7-1 or PD-L1 to cell surface PD-L1 or B7-1, respectively, is only likely to occur when the local concentration is high enough to compete with the cell surface binding. This may occur under nonphysiologic or pathologic conditions (24–28). In addition, the B7-1–PD-L1 interaction has been reported to regulate the graft versus leukemia activity of donor T cells (29). Much remains to be learned about the pathway's mechanism and downstream signaling.

Some other cell surface receptors can bind ligands both *in trans* and *in cis* (30). One example is the engagement of TNF family receptor herpes virus entry mediator (HVEM) with its ligand, B- and T-lymphocyte attenuator (BTLA). Interaction of HVEM with

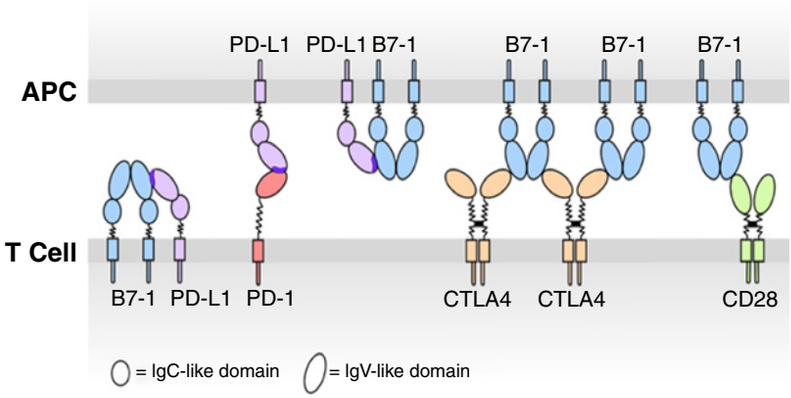

Figure 7.

Model for PD-L1 binding to B7-1 *in cis*. Cell surface PD-L1 interacts with cell surface PD-1 *in trans* but not with cell surface B7-1 *in trans.* Cell surface PD-L1 can interact with cell surface B7-1 *in cis*. B7-1 can interact with CTLA4 or CD28 *in trans*.

BTLA *in trans* delivers bidirectional signals, which costimulate HVEM-expressing cells while coinhibiting BTLA-expressing cells. However, HVEM interacting with BTLA *in cis* inhibits the *trans* HVEM interaction, and this *cis* interaction may participate in maintenance of T cells in the naive state (31). Binding *in cis* is generally functionally inert and serves as a competitive inhibitor for the functional binding *in trans*. Thus, a *cis* interaction modifies the threshold for a response to occur (30). The work by Haile and colleagues is compatible with the structural orientation of PD-L1 and B7-1, allowing binding *in cis* on the same cell or of soluble B7-1 to cell surface PD-L1 (20–22). Although some cell surface molecules bind the same receptor or ligand both *in trans* and *in cis*, the possibilities for PD-L1 are more restricted. PD-L1 binds PD-1 *in trans* and B7-1 *in cis*, and binding to B7-1 competes with binding to PD-1.

Binding *in cis* may be facilitated via a long flexible stalk region, a reversal of the orientation of domains, or symmetric binding sites (30). A previous study analyzed the evolutionary history of T-cell costimulatory molecules and found that many of the positively selected sites in PD-L1 and PD-L2 are in the stalk domain (32). Positively selected sites in the stalk of PD-L1 might modulate the capacity of PD-L1 to bend and assume an optimal positioning to form *cis* interactions with B7-1 on the same cell surface (33). This supports our model that PD-L1 can bend via the flexible stalk to bind to B7-1 *in cis*.

Our data also support previous findings that coexpression of B7-1 on PD-L1$^+$ human tumor cells rendered PD-L1 undetectable by PD-1-Fc and by some human PD-L1 mAbs (29E.2A3, MIH1, and 27A2) although still detectable by 5H1 mAb (21, 22). This result may be explained by B7-1 binding to PD-L1 sterically blocking the epitopes recognized by some antibodies (21).

Our data support the previous report of binding of both B7-1 and PD-1 to PD-L1 in the same vicinity (18). In line with this, we see a requirement for only the IgV domain of PD-L1 for binding with PD-1 and B7-1 (18). The evolutionary conservation and concentration-dependent blocking of PD-L1 interaction with B7-1 by PD-L1 antibodies also suggests the binding to be functionally relevant rather than a chance homology binding. Some studies have shown that B7-1 competes with PD-1 for binding to PD-L1 (20–22). We performed competition assays and showed that PD-1 and B7-1 competed for binding to PD-L1 and could block each other's binding. Thus, the PD-L1–B7-1 interaction affects the interplay of costimulatory molecular pathways. We propose that the end result of competing *cis* and *trans* interactions would be based on the number of B7-1 or PD-1 molecules available on local cell surfaces to bind with PD-L1. It remains unknown whether other costimulatory pathways are affected. Our coexpression data in tumor-infiltrating myeloid cells further support the biological significance of the interaction and are in line with previous findings of PD-L1 expression on tumor-infiltrating macrophages (34).

Our results change the current understanding of the interaction between PD-L1 and B7-1 and suggest avenues for a more targeted therapy approach. Our results help to better understand the biology of the PD-1–PD-L1 pathway, the mechanisms for the antibody blockade of PD-L1 and PD-1, and potential applications of blockade of B7-1 or soluble B7-1 administration.

In summary, the structural and binding features of PD-L1 and B7-1 shown here indicate that coexpression of B7-1 and PD-L1 and their interaction *in cis* may help coordinate the binding of shared ligands or receptors to optimize the limited space between two cells and modulate cellular functions. Binding of PD-L1 to B7-1 *in cis* may also render PD-L1 unavailable to PD-1 and some PD-L1 mAbs. Our findings may inform strategies to use PD-L1 and B7-1 pathways to overcome PD-L1–mediated immunosuppression in cancer immunotherapy.

Disclosure of Potential Conflicts of Interest

G.J. Freeman has ownership interest in Bristol-Myers Squibb, Merck, Roche, EMD-Serono, Boehringer-Ingelheim, Amplimmune, Dako, and Novartis and is a consultant/advisory board member for Bristol-Myers Squibb, Xios, Surface Oncology, Novartis, Elstar, SQ2 Biotech, Adaptimmune, and OrigiMed. No potential conflicts of interest were disclosed by the other authors.

Authors' Contributions

Conception and design: G.J. Freeman, A. Chaudhri, Y. Xiao, A.N. Klee
Development of methodology: G.J. Freeman, A. Chaudhri, Y. Xiao, A.N. Klee
Acquisition of data (provided animals, acquired and managed patients, provided facilities, etc.): G.J. Freeman, A. Chaudhri, Y. Xiao, A.N. Klee, X. Wang, B. Zhu
Analysis and interpretation of data (e.g., statistical analysis, biostatistics, computational analysis): G.J. Freeman, A. Chaudhri, Y. Xiao, A.N. Klee, X. Wang, B. Zhu
Writing, review, and/or revision of the manuscript: G.J. Freeman, A. Chaudhri, Y. Xiao, A.N. Klee
Administrative, technical, or material support (i.e., reporting or organizing data, constructing databases): Y. Xiao
Study supervision: G.J. Freeman

Acknowledgments

This work was supported by NIH grants P01 AI056299, R01 AI089955, P01 AI054456, and HHSN272201100018C (to G.J. Freeman).

The costs of publication of this article were defrayed in part by the payment of page charges. This article must therefore be hereby marked *advertisement* in accordance with 18 U.S.C. Section 1734 solely to indicate this fact.

Received June 20, 2017; revised February 19, 2018; accepted June 1, 2018; published first June 5, 2018.

References

1. Topalian SL, Hodi FS, Brahmer JR, Gettinger SN, Smith DC, McDermott DF, et al. Safety, activity, and immune correlates of anti-PD-1 antibody in cancer. N Engl J Med 2012;366:2443–54.
2. Powles T, Eder JP, Fine GD, Braiteh FS, Loriot Y, Cruz C, et al. MPDL3280A (anti-PD-L1) treatment leads to clinical activity in metastatic bladder cancer. Nature 2014;515:558–62.
3. Dong H, Strome SE, Salomao DR, Tamura H, Hirano F, Flies DB, et al. Tumor-associated B7-H1 promotes T-cell apoptosis: a potential mechanism of immune evasion. Nat Med 2002;8:793–800.
4. Latchman YE, Liang SC, Wu Y, Chernova T, Sobel RA, Klemm M, et al. PD-L1-deficient mice show that PD-L1 on T cells, antigen-presenting cells, and host tissues negatively regulates T cells. Proc Natl Acad Sci USA 2004;101:10691–6.
5. Freeman GJ, Long AJ, Iwai Y, Bourque K, Chernova T, Nishimura H, et al. Engagement of the PD-1 immunoinhibitory receptor by a novel B7 family member leads to negative regulation of lymphocyte activation. J Exp Med 2000;192:1027–34.
6. Azuma T, Yao S, Zhu G, Flies AS, Flies SJ, Chen L. B7-H1 is a ubiquitous antiapoptotic receptor on cancer cells. Blood 2008;111:3635–43.
7. Rodig N, Ryan T, Allen JA, Pang H, Grabie N, Chernova T, et al. Endothelial expression of PD-L1 and PD-L2 down-regulates CD8+ T cell activation and cytolysis. Eur J Immunol 2003;33:3117–26.

8. Francisco LM, Salinas VH, Brown KE, Vanguri VK, Freeman GJ, Kuchroo VK, et al. PD-L1 regulates the development, maintenance, and function of induced regulatory T cells. J Exp Med 2009;206:3015–29.
9. Butte MJ, Keir ME, Phamduy TB, Sharpe AH, Freeman GJ. Programmed death-1 ligand 1 interacts specifically with the B7–1 costimulatory molecule to inhibit T cell responses. Immunity 2007;27:111–22.
10. Butte MJ, Pena-Cruz V, Kim MJ, Freeman GJ, Sharpe AH. Interaction of human PD-L1 and B7–1. Mol Immunol 2008;45:3567–72.
11. Park JJ, Omiya R, Matsumura Y, Sakoda Y, Kuramasu A, Augustine MM, et al. B7-H1/CD80 interaction is required for the induction and maintenance of peripheral T-cell tolerance. Blood 2010;116:1291–8.
12. Cheng X, Veverka V, Radhakrishnan A, Waters LC, Muskett FW, Morgan SH, et al. Structure and interactions of the human programmed cell death 1 receptor. J Biol Chem 2013;288:11771–85.
13. Xiao Y, Yu S, Zhu B, Bedoret D, Bu X, Francisco LM, et al. RGMb is a novel binding partner for PD-L2 and its engagement with PD-L2 promotes respiratory tolerance. J Exp Med 2014;211:943–59.
14. Latchman Y, Wood CR, Chernova T, Chaudhary D, Borde M, Chernova I, et al. PD-L2 is a second ligand for PD-1 and inhibits T cell activation. Nature Immunol 2001;2:261–8.
15. Brown JA, Dorfman DM, Ma FR, Sullivan EL, Munoz O, Wood CR, et al. Blockade of programmed death-1 ligands on dendritic cells enhances T cell activation and cytokine production. J Immunol 2003;170:1257–66.
16. Zhu B, Cai G, Hall EO, Freeman GJ. In-fusion assembly: seamless engineering of multidomain fusion proteins, modular vectors, and mutations. BioTechniques 2007;43:354–9.
17. Lin DY, Tanaka Y, Iwasaki M, Gittis AG, Su HP, Mikami B, et al. The PD-1/PD-L1 complex resembles the antigen-binding Fv domains of antibodies and T cell receptors. Proc Natl Acad Sci USA 2008;105:3011–6.
18. Paterson AM, Brown KE, Keir ME, Vanguri VK, Riella LV, Chandraker A, et al. The programmed death-1 ligand 1:B7–1 pathway restrains diabetogenic effector T cells in vivo. J Immunol 2011;187:1097–105.
19. Yang J, Riella LV, Chock S, Liu T, Zhao X, Yuan X, et al. The novel costimulatory programmed death ligand 1/B7.1 pathway is functional in inhibiting alloimmune responses in vivo. J Immunol 2011;187:1113–9.
20. Haile ST, Horn LA, Ostrand-Rosenberg S. A soluble form of CD80 enhances antitumor immunity by neutralizing programmed death ligand-1 and simultaneously providing costimulation. Cancer Immunol Res 2014;2:610–5.
21. Haile ST, Dalal SP, Clements V, Tamada K, Ostrand-Rosenberg S. Soluble CD80 restores T cell activation and overcomes tumor cell programmed death ligand 1-mediated immune suppression. J Immunol 2013;191:2829–36.
22. Haile ST, Bosch JJ, Agu NI, Zeender AM, Somasundaram P, Srivastava MK, et al. Tumor cell programmed death ligand 1-mediated T cell suppression is overcome by coexpression of CD80. J Immunol 2011;186:6822–9.
23. Taylor PA, Lees CJ, Fournier S, Allison JP, Sharpe AH, Blazar BR. B7 expression on T cells down-regulates immune responses through CTLA-4 ligation via T-T interactions. J Immunol 2004;172:34–9.
24. Wan B, Nie H, Liu A, Feng G, He D, Xu R, et al. Aberrant regulation of synovial T cell activation by soluble costimulatory molecules in rheumatoid arthritis. J Immunol 2006;177:8844–50.
25. Shi B, Du X, Wang Q, Chen Y, Zhang X. Increased PD-1 on CD4(+)CD28(-) T cell and soluble PD-1 ligand-1 in patients with T2DM: association with atherosclerotic macrovascular diseases. Metabolism 2013;62:778–85.
26. Rossille D, Gressier M, Damotte D, Maucort-Boulch D, Pangault C, Semana G, et al. High level of soluble programmed cell death ligand 1 in blood impacts overall survival in aggressive diffuse large B-cell lymphoma: results from a French multicenter clinical trial. Leukemia 2014;28:2367–75.
27. Frigola X, Inman BA, Krco CJ, Liu X, Harrington SM, Bulur PA, et al. Soluble B7-H1: differences in production between dendritic cells and T cells. Immunol Lett 2012;142:78–82.
28. Frigola X, Inman BA, Lohse CM, Krco CJ, Cheville JC, Thompson RH, et al. Identification of a soluble form of B7-H1 that retains immunosuppressive activity and is associated with aggressive renal cell carcinoma. Clin Cancer Res 2011;17:1915–23.
29. Ni X, Song Q, Cassady K, Deng R, Jin H, Zhang M, et al. PD-L1 interacts with CD80 to regulate graft-versus-leukemia activity of donor CD8+ T cells. J Clin Invest 2017;127:1960–77.
30. Held W, Mariuzza RA. Cis-trans interactions of cell surface receptors: biological roles and structural basis. Cell Mol Life Sci 2011;68:3469–78.
31. Cheung TC, Oborne LM, Steinberg MW, Macauley MG, Fukuyama S, Sanjo H, et al. T cell intrinsic heterodimeric complexes between HVEM and BTLA determine receptivity to the surrounding microenvironment. J Immunol 2009;183:7286–96.
32. Forni D, Cagliani R, Pozzoli U, Colleoni M, Riva S, Biasin M, et al. A 175 million year history of T cell regulatory molecules reveals widespread selection, with adaptive evolution of disease alleles. Immunity 2013;38:1129–41.
33. Jones JC, Freeman GJ. Costimulatory genes: hotspots of conflict between host defense and autoimmunity. Immunity 2013;38:1083–5.
34. Hartley G, Regan D, Guth A, Dow S. Regulation of PD-L1 expression on murine tumor-associated monocytes and macrophages by locally produced TNF-alpha. Cancer Immunol Immunother 2017;66:523–35.